(3) Abrams, D. S.; Prausnitz, J. M. *AIChE J.* **1975**, *21*, 116.
(4) Klaus, R. L.; Van Ness, H. C. *AIChE J.* **1967**, *13*, 1132.
(5) Sørensen, J. M.; Magnussen, T.; Rasmussen, P.; Fredenslund, Aa. *Fluid Phase Equilib* **1979**, *3*, 47.
(6) Hand, D. B. *J. Phys. Chem.* **1930**, *34*, 1961.
(7) Wilhoit, R. C.; Zwolinski, B. J. "Physical and Thermodynamic Properties of Aliphatic Alcohols"; American Chemical Society: Washington, DC, 1973; *J. Phys. Chem. Ref. Data, Suppl. 1*, Vol. 2.
(8) Dreisbach, R. R. "Physical Properties of Chemical Substances"; Dow Chemical Co.: Midland, MI, 1952.

Received for review August 9, 1982. Revised manuscript received February 3, 1984. Accepted March 12, 1984. Funds for this work was provided by the "Dirección General de Desarrollo Científico y Técnológico", Universidad Técnica Federico Santa María, Chile.

Fluid Phase Equilibria for the System Dimethyl Ether/Water from 50 to 220 °C and Pressures to 50.9 MPa

Maria E. Pozo and William B. Streett*

School of Chemical Engineering, Cornell University, Ithaca, New York 14853

Experimental studies of vapor–liquid, vapor–liquid–liquid, and liquid–liquid equilibria in the system dimethyl ether/water (DME/H_2O) have been carried out at 14 temperatures in the range 50–220 °C and pressures up to 50.9 MPa. The data have been obtained by using a vapor-recirculating apparatus operating at isothermal conditions. The phase diagram for this system exhibits a three-phase region of vapor–liquid–liquid equilibrium, ending at an upper critical end point where the vapor phase and the DME-rich liquid phase become identical. The mixture critical line consists of two branches. One begins at the critical point of pure dimethyl ether (126.9 °C and 5.27 MPa) and ends at the upper critical end point (157.0 °C and 6.72 MPa). The other branch begins at the critical point of pure water (374.2 °C and 22.09 MPa) as a liquid–vapor critical line and merges into a liquid–liquid critical line that rises sharply in pressure as the temperature drops below that of the upper critical end point.

Introduction

This is the third in a series of reports of vapor–liquid equilibrium (VLE) studies of binary mixtures containing dimethyl ether ($(CH_3)_2O$, DME), carbon dioxide (CO_2), methanol (CH_3OH), and water (H_2O). VLE data for the systems CO_2/DME, DME/CH_3OH have been reported (*1*, *2*).

Phase equilibrium data for these systems are needed to support the development of the Mobil process for converting methanol to gasoline (*3*, *4*). These studies will also provide data to be used for testing and refining data prediction methods based on statistical mechanics and intermolecular potential theory (*5*).

This report presents the tabulated experimental data and describes the principal quantitative and qualitative features of the $P-T-X-Y$ phase diagram. A brief qualitative description of the phase diagram has been published separately (*6*).

Experimental Section

The essential features of the apparatus and method were similar to those used in earlier studies of CO_2/DME (*1*) and DME/methanol (*2*). A vapor-recirculating equilibrium system was used, and measurements of the compositions of coexisting liquid and vapor phases were made as functions of pressure at selected fixed temperatures. The earlier papers (*1*, *2*) should be consulted for general details of the method.

To facilitate the DME/H_2O experiments described here, several changes were made in the apparatus. The most important of these were the following: (1) the use of windowed cells at low to moderate pressures (up to 29 MPa) to provide visual observation of the mixture in the three-phase region and along the critical line; and (2) the use of a separately heated sampling chamber to ensure the complete vaporization of samples withdrawn from the liquid phase.

To facilitate observation of the mixtures the heated oil bath previously used for temperature control was replaced by a commercial windowed oven (Blue M Co. Blue Island, IL) suitable for use at temperatures up to 250 °C. The oven uses forced convection and horizontal air flow and is capable of maintaining temperatures constant to within ±0.02 °C, with no significant gradients in the region of the equilibrium system.

A diagram of the modified apparatus is shown in Figure 1. The heart of the system is the equilibrium cell A, coupled to the magnetically operated pump C, by $^1/_8$ in. o.d. stainless steel tubing to form a closed loop (shown by the dark lines). The action of the pump withdraws the least dense phase from the top of the cell and recirculates it around the closed loop, so that it bubbles through the remaining phase (or phases) in the lower part of the cell. This bubbling action provides intimate contact between phases and promotes a rapid approach to equilibrium, which is usually reached in 10–15 min. The recirculating system works equally well for studies of liquid–vapor, liquid–liquid–vapor, or liquid–liquid phase equilibrium. In the latter case the less dense liquid phase (the DME-rich phase) is bubbled through the more dense, H_2O-rich liquid phase.

At low pressures, up to about 8 MPa, we used an equilibrium cell made of extra heavy wall Pyrex tubing, confined between stainless steel flanges and sealed by Teflon O rings. This provided complete visibility of the mixture and was especially useful as an aid to sampling in the three-phase region. It also provided interesting views of critical opalescence at the DME-rich end of the vapor–liquid critical line. At intermediate pressures (up to about 29 MPa) we used a windowed cell of experimental design, fitted with several small windows of synthetic sapphire. The window seals developed leaks at high pressures and temperatures, so we switched finally to an all stainless steel cell for the remaining studies of the liquid–liquid region at high pressures.

In previous experiments on CO_2/DME and DME/methanol, samples were withdrawn through heated capillary sampling lines and passed directly into the gas sampling valve of a gas chromatograph. In this work we found that cooling effects, resulting from throttling the liquid samples to low pressure through the sampling valves, caused partial condensation of the

0021-9568/84/1729-0324$01.50/0 © 1984 American Chemical Society

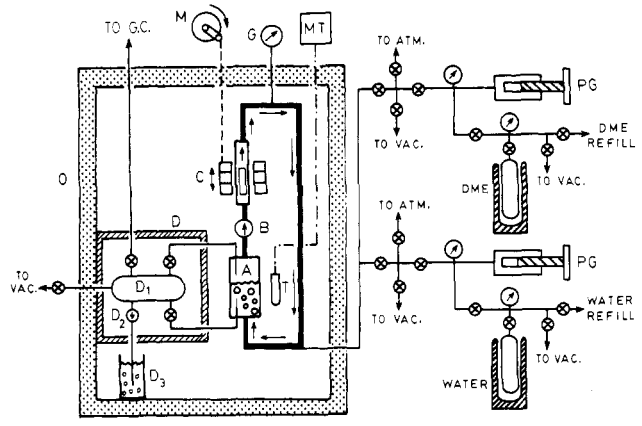

Figure 1. Schematic diagram of the vapor-recirculating apparatus: equilibrium cell (A), check valve (B), magnetically operated pump (C), motor with mechanical linkage (M), heated chamber (D), sampling cell (D_1), 25 psig pressure relief valve (D_2), oil container (D_3), pressure gauge (G), temperature-controlled oven (O), platinum resistance thermometer (T), Mueller bridge (MT). DME and H_2O are distilled from stainless steel cylinder into the hand-operated pressure generators (PG), which can reach pressures up to 100 MPa.

H_2O, resulting in separation of the components before the sample reached the gas chromatograph. To overcome this problem the sampling valves, together with a low-pressure sampling cell D_1, were placed in an insulated and separately heated chamber D, inside the oven O (see Figure 1), and heated to a temperature of 150 °C or higher (at least 20 °C above the oven temperature). The liquid sample was withdrawn into the previously evacuated sampling cell D_1, where it was allowed to stand for sufficient time to vaporize and become fully mixed (about 10 min) before being injected into the sampling valve of the gas chromatograph. The sampling cell was fitted with a 25 psig pressure relief valve D_2, with an outlet line inserted into a small beaker of oil D_3, to serve as an overflow and to indicate when the sampling cell was filled to a pressure of 25 psig. The heated sampling valves were fitted with long stems that passed through the oven wall to permit remote operation. The sampling line between the sample cell and the gas chromatograph was heated to 150 °C.

Temperatures were measured by a platinum resistance thermometer T and Mueller bridge MT and are accurate to ±0.02 °C. Pressures were measured with an uncertainty of ±0.007 MPa or ±0.5% (whichever is greater) by an Autoclave Model DPS pressure gauge G calibrated in this laboratory against a Ruska dead-weight gauge.

Gas samples were analyzed with a programmable gas chromatograph, Hewlett-Packard Model 5840 A, with thermal conductivity detector, a built-in digital process control, and an automatic sampling valve. A satisfactory separation of DME and H_2O was obtained by using helium as a carrier gas at 25 cm^3/min and a 6 ft long column of 80/100 mesh Porapak-QS, packed in $^1/_8$ in. o.d. stainless steel tubing. The column operating temperature was set at 140 °C, with a 30 °C/min temperature rise following the emergence of the water peak to accelerate the passage of DME through the column. The gas chromatograph was calibrated by mixtures of known compositions prepared by weight.

The phase compositions reported here are estimated to be accurate within ±0.3 mol %, except near the critical line where the uncertainty may be as large as 1%.

The DME used in this work was supplied by Ideal Gas Products, Inc. (Edison, NJ), and had an initial purity of 99.5%, where the major contaminants were methanol, carbon dioxide, and methyl formate. After the DME was distilled under vacuum, no measurable impurities were observed in a chromatographic trace analysis. The final purity was estimated to be 99.9% or better. The water used in this work was demineralized by using an Ion-exchange unit and degassed by boiling under a partial vacuum.

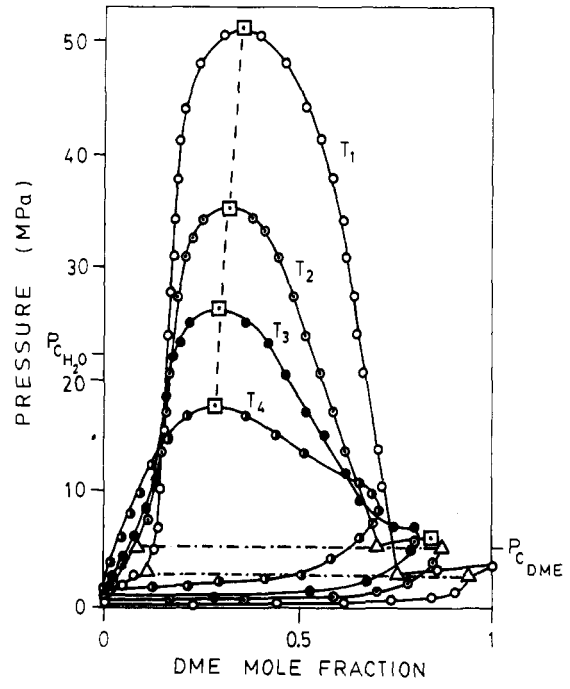

Figure 2. Pressure–composition diagram for the system DME/H_2O: T_1 = 100.11 °C, T_2 = 140.85 °C, T_3 = 160.05 °C, T_4 = 200.45 °C; (△) three-phase line; (□) mixture critical point; (--□--) high-pressure critical line; ($P_{C_{DME}}$) critical pressure of pure dimethyl ether; ($P_{C_{H_2O}}$) critical pressure of pure water.

Results

Compositions of the coexisting phases have been measured at 14 temperatures from 50.00 to 220.01 °C and at pressures up to 50.9 MPa. The results are tabulated in Tables I–VI.

The following notation has been used throughout the tables in order to facilitate the data display: L^α is the liquid phase rich in water; L^β is the liquid phase rich in DME; X_i^α and X_i^β are the mole fractions of component i in the liquid phases; Y_i is the mole fraction of component i in the vapor phase; and the subscripts i = 1 and i = 2 refer to DME and H_2O, respectively.

Three types of isotherms were found in the range covered in this study. Isotherms below the critical temperature of DME (126.9 °C) have a three-phase point and three separate two-phase regions: L^α + V, L^β + V, and L^α + L^β. The latter is bounded at high pressures by a critical point. Isotherms between the DME critical point and the upper critical end point (UCEP, 157 °C) also have a three-phase point and the same three two-phase regions; however, two of these (L^β + V and L^α + L^β) end at high pressures in critical points. The third type of isotherm, at temperatures above the UCEP, exhibits only L^α + V equilibrium, ending at high pressures in a critical point. (See Figure 6.)

Description of the Phase Diagram

Four isotherms from the experimental data are plotted on a P–X diagram in Figure 2. K-value plots for three of these ($K \equiv Y_i/X_i$) are shown on a log K vs. log P diagram in Figure 3. These are representative of the three types of isotherms described in the preceding paragraph. (See also Figure 6.)

The DME/H_2O system exhibits a liquid–liquid phase separation and a mixture critical line that has two separate branches. It is a class III system in the phase equilibrium classification scheme of Van Konynenburg and Scott (7). A schematic three-dimensional drawing of the DME/H_2O phase diagram is shown in Figure 4. In this diagram the dark solid lines AC_2 and

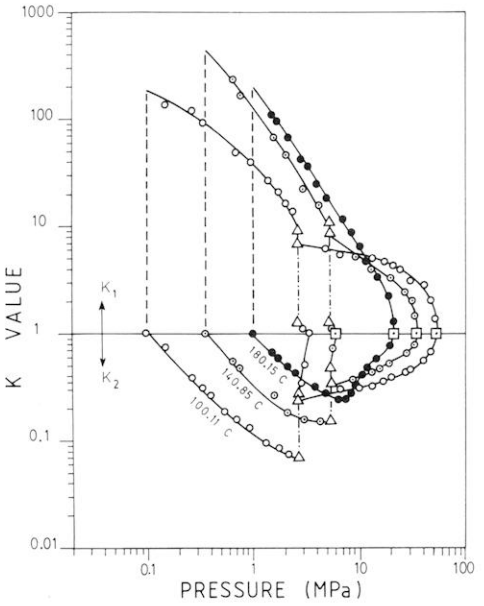

Figure 3. K value vs. pressure plots for three types of isotherms: K_1, K value for DME; K_2, K value for H_2O; (△) three-phase line; (□) mixture critical point.

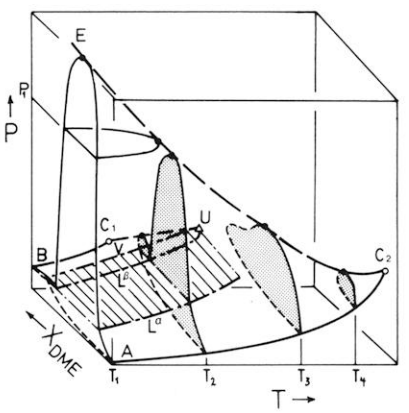

Figure 4. Schematic three-dimensional drawing of the $P-T-X-Y$ phase diagram for DME/H_2O. C_1 and C_2 are the critical points of pure DME and H_2O, respectively, and U is the upper critical end point. The four vertical planes, T_1, T_2, T_3, and T_4, are isotherms; three are shaded, but the fourth, T_1, has been left unshaded in the interest of clarity. The horizontal plane P_1 (unshaded) is an isobar. The line E–C_2 is the high-pressure critical line of the mixture, and the line C_1–U is the low-pressure critical line of the mixture. (See text for further description.)

BC_1 are the vapor pressure curves of H_2O and DME, respectively, lying in the two PT faces of the diagram. C_2 and C_1 are the critical points of H_2O and DME. The region of coexistence of three phases, liquid–liquid–vapor, is defined by the three dash–dot lines L^α, L^β, and V. The branch of the critical line that extends into the diagram from the DME critical point, C_1 (126.9 °C, 5.27 MPa), ends at the upper critical end point U (157 °C, 6.72 MPa, 79 mol % DME) where it intersects the three-phase region. The second branch extends into the diagram from the H_2O critical point C_2 (374.2 °C, 22.09 MPa) and passes through a minimum in pressure before rising sharply to high pressures with decreasing temperature; it presumably ends at higher pressures and lower temperatures, beyond the range of these experiments, where a solid phase of H_2O appears.

The upper critical end point U is a limiting point in the three-phase region, at which two of the phases (L^β and V) become identical in the presence of the third phase (L^α). At temperatures above that of U there is only one liquid phase (the H_2O-rich liquid, L^α). It follows from geometrical constraints imposed by the phase rule, and by the choice of variables

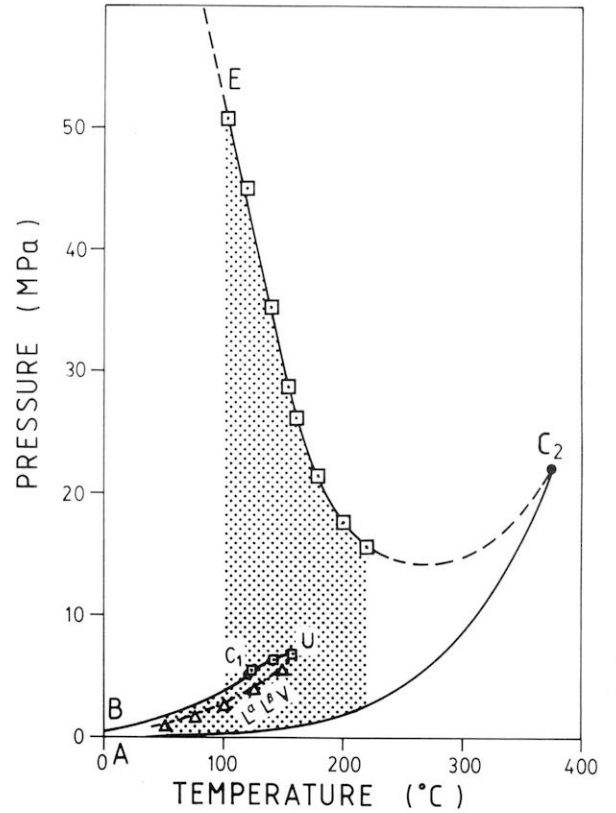

Figure 5. Pressure–temperature diagram for the system DME/H_2O. In this figure the principal boundary lines of Figure 4 (vapor pressure curves, critcal lines, three-phase lines) are projected on a $P-T$ plane. The shaded area is the region of $P-T$ space covered in the experiment.

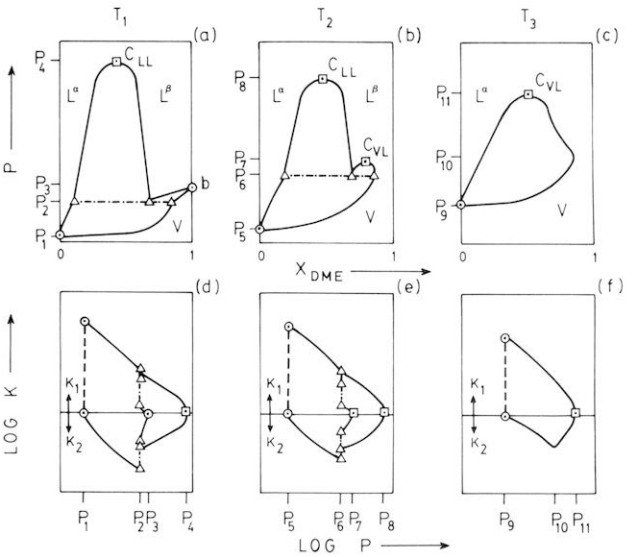

Figure 6. Pressure–composition and K value–pressure diagrams showing the qualitative features of isotherms in different parts of the phase diagram. Symbols as in Figures 2 and 3. (See text for discussion.)

(pressure, temperature, composition), that the lines representing three coexisting phases, L^α, L^β, and V, lie in a ruled surface (the one shaded by parallel lines in Figure 4) that is perpendicular to the $P-T$ coordinate planes. These lines therefore appear as a single line in a $P-T$ projection of the three-dimensional diagram. A $P-T$ projection drawn from the experimental data is shown in Figure 5. That portion of the mixture critical line between the critical point C_2 of H_2O and the highest experimental temperature, 220 °C, has not been measured, and its location is not precisely known. It is clear from the available

Table I. Experimental Equilibrium Compositions for DME/H_2O[a] in the Vapor-Liquid (L^α) Region

P, MPa	X_1[a]	Y_1	P, MPa	X_1[a]	Y_1	P, MPa	X_1[a]	Y_1	P, MPa	X_1[a]	Y_1
		T = 50.00 °C						T = 160.05 °C			
0.012	0.000	0.000	0.407	0.041	0.956	0.618	0.000	0.000	7.067	0.091	0.776
0.138		0.894	0.448	0.045	0.957	1.048		0.424	7.198		0.751
0.152		0.900	0.552	0.051	0.964	1.165	0.002	0.448	7.736	0.103	0.701
0.193		0.922	0.765	0.085	0.965	1.393	0.006	0.523	8.287	0.107	0.681
0.248		0.934	0.834	0.098	0.967	1.737	0.009	0.615	8.963	0.111	0.667
0.310	0.028	0.945	1.027	0.155	0.977	2.110	0.010	0.667	9.653	0.119	0.653
		T = 75.00 °C				2.510	0.015	0.687	11.721	0.133	0.621
0.039	0.000	0.000	0.552	0.019	0.913	3.103	0.024	0.732	13.996	0.140	0.584
0.145		0.655	0.807	0.028	0.933	3.820	0.032	0.752	17.306	0.146	0.518
0.186		0.739	0.945	0.043	0.941	3.958		0.762	20.795	0.171	0.468
0.228		0.773	1.324	0.071	0.956	4.151	0.045	0.774	23.621	0.197	0.418
0.283		0.823	1.593	0.087	0.957	5.171	0.060	0.788	25.235	0.211	0.365
0.324	0.011	0.850	1.800	0.128	0.958	6.164	0.078	0.809	25.959	0.240	0.318
0.400	0.015	0.878				6.543	0.083	0.823	(26.3)	(0.29)	(0.29)
		T = 100.11 °C				6.888		0.824			
0.101	0.000	0.000	0.717	0.018	0.841			T = 180.15 °C			
0.138		0.228	0.979	0.021	0.872	1.002	0.000	0.000	6.205	0.057	0.762
0.152		0.269	1.372	0.034	0.905	1.117		0.113	6.964	0.070	0.764
0.200		0.441	1.744	0.044	0.915	1.193	0.001	0.167	7.605	0.078	0.774
0.276		0.612	2.062	0.054	0.925	1.338	0.002	0.257	8.977	0.090	0.730
0.345	0.007	0.684	2.441	0.065	0.931	1.517	0.003	0.332	9.398	0.096	0.691
0.414		0.732	2.848	0.104	0.936	1.669	0.004	0.376	9.680	0.099	0.674
0.565	0.008	0.803				1.875	0.005	0.430	10.342	0.110	0.639
		T = 121.06 °C				2.082	0.007	0.482	11.087	0.114	0.616
0.206	0.000	0.000	1.110	0.013	0.785	2.399	0.008	0.536	12.548	0.134	0.578
0.262		0.180	1.379	0.019	0.818	2.758	0.014	0.586	15.334	0.153	0.517
0.296		0.279	1.779	0.026	0.852	3.206	0.018	0.634	15.975	0.164	0.498
0.372		0.429	2.220	0.031	0.871	3.447	0.021	0.655	18.243	0.183	0.416
0.476		0.549	2.620	0.043	0.881	3.820	0.026	0.676	18.988	0.197	0.411
0.496	0.004	0.563	2.861	0.048	0.884	4.137	0.031	0.701	20.477	0.219	0.382
0.731	0.007	0.697	3.565	0.069	0.899	4.868	0.039	0.723	21.098	0.258	0.328
0.910	0.012	0.749	4.054	0.090	0.910	5.557	0.046	0.750	(21.4)	(0.28)	(0.28)
		T = 130.11 °C						T = 200.45 °C			
0.270	0.000	0.000	0.945	0.008	0.687	1.553	0.000	0.000	7.819	0.062	0.696
0.296		0.079	1.014	0.010	0.705	1.627		0.129	8.412	0.069	0.703
0.338		0.190	1.282	0.012	0.745	1.662		0.148	9.660	0.086	0.706
0.365		0.250	1.772	0.020	0.811	1.765	0.001	0.207	10.494	0.098	0.681
0.441		0.367	2.427	0.029	0.835	1.834	0.002	0.215	11.135	0.102	0.653
0.496		0.438	3.116	0.040	0.863	2.165	0.003	0.291	11.928	0.117	0.600
0.586	0.003	0.518	3.709	0.053	0.875	2.496	0.007	0.414	12.514	0.141	0.577
0.724	0.005	0.611	4.123	0.067	0.877	3.185	0.012	0.512	13.927	0.143	0.505
0.779		0.639	4.661	0.087	0.879	3.654	0.017	0.543	14.500	0.153	0.466
0.848	0.006	0.662				4.275	0.020	0.580	15.306	0.164	0.443
		T = 140.85 °C				5.033	0.027	0.619	16.285	0.198	0.405
0.367	0.000	0.000	1.338	0.010	0.683	5.792	0.046	0.656	17.306	0.225	0.310
0.400		0.090	1.655	0.011	0.741	6.550	0.048	0.662	(17.6)	(0.27)	(0.27)
0.441		0.167	2.137	0.017	0.784	7.171	0.052	0.678			
0.462		0.203	3.061	0.027	0.817			T = 220.01 °C			
0.524		0.303	3.709	0.035	0.845	2.318	0.000	0.000	10.218	0.074	0.623
0.579	0.001	0.355	4.351	0.051	0.854	2.827	0.001	0.151	10.728	0.077	0.605
0.662	0.002	0.441	4.895	0.067	0.859	3.434	0.003	0.252	11.032	0.082	0.578
0.758	0.003	0.508	5.454	0.081	0.862	4.151	0.007	0.362	11.280	0.088	0.554
0.979	0.004	0.590				4.840	0.010	0.456	12.390	0.103	0.502
		T = 150.35 °C				5.502	0.013	0.532	13.100	0.119	0.457
0.476	0.000	0.000	2.055	0.017	0.710	6.860	0.026	0.607	13.838	0.139	0.415
0.614		0.211	2.206	0.018	0.724	7.143	0.040	0.613	14.527	0.165	0.377
0.683		0.297	2.558	0.025	0.757	7.791	0.047	0.629	14.824	0.176	0.368
0.745		0.342	3.172	0.033	0.783	9.101	0.052	0.649	(15.5)	(0.26)	(0.26)
0.841		0.404	3.765	0.040	0.808	9.687	0.059	0.663			
1.034	0.005	0.493	4.399	0.054	0.812						
1.117	0.006	0.520	5.130	0.056	0.829						
1.351	0.008	0.592	5.819	0.082	0.839						
1.586	0.012	0.643	6.219	0.093	0.844						

[a] The pure-component vapor pressures have been obtained from the literature (8). The mixture critical points (enclosed in parentheses) have been estimated by extrapolation of the experimental measurements.

experimental data that it must have a pressure minimum between 220 °C and the H_2O critical point (374.2 °C), and it may have a pressure maximum as well. The three-phase line in Figure 5 is the $P-T$ projection of the three separate lines L^α, L^β, and V in Figure 4. Because it appears as a single line on $P-T$ diagram, it is sometimes called the "three-phase line"; however, this is slightly misleading, because there are three separate lines in $P-T-X$ space. That they have a common projection on a PT diagram is a consequence of the fact that P and T are "field" variables—that is, variables that are the

Table II. Experimental Equilibrium Compositions for DME/H_2O[a] in the Vapor-Liquid (L^β) Region

P, MPa	X_1^β	Y_1	P, MPa	X_1^β	Y_1
		T = 50.00 °C			
1.027	0.814	0.977	1.177	0.977	0.922
1.041	0.817	0.978	1.152	1.000	1.000
1.082	0.920	0.984			
		T = 75.00 °C			
1.800	0.781	0.958	2.020	0.991	0.994
1.882	0.907	0.972	2.036	1.000	1.000
		T = 100.11 °C			
2.848	0.755	0.936	3.110	0.934	0.967
2.861	0.777	0.941	3.257	1.000	1.000
2.958	0.855	0.950			
		T = 121.06 °C			
4.054	0.727	0.910	4.399	0.898	0.938
4.151	0.806	0.918	4.606	0.949	0.969
4.220	0.851	0.922	4.735	1.000	1.000
		T = 127.34 °C			
4.440	0.725	0.901	5.226	0.970	0.972
4.661	0.843	0.918	5.261	0.976	0.978
4.895	0.902	0.936	(5.3)	(0.98)	(0.98)
5.199	0.965	0.970			
		T = 130.11 °C			
4.661	0.721	0.879	5.081	0.885	0.919
4.709	0.778	0.890	5.226	0.917	0.936
4.813	0.819	0.895	5.330	0.936	0.948
5.012	0.871	0.915	(5.4)	(0.95)	(0.95)
		T = 140.85 °C			
5.454	0.705	0.862	5.909	0.852	0.873
5.681	0.803	0.874	5.929	0.866	0.872
5.805	0.829	0.876	(5.9)	(0.87)	(0.87)
		T = 150.35 °C			
6.219	0.736	0.844	6.419	0.815	0.834
6.281	0.764	0.845	(6.4)	(0.82)	(0.82)
6.391	0.794	0.841			
		T = 154.25 °C			
6.605	0.755	0.832	6.647	0.773	0.817
6.633	0.759	0.822	(6.6)	(0.79)	(0.79)

[a] The pure-component vapor pressures are from the literature (9). Mixture critical points (in parentheses) have been estimated by extrapolation of experimental measurements.

same for all phases in equilibrium.

Three different types of isotherms appear in Figure 4, and these are shown separately in Figure 6a–c as projections on a P–X diagram. (The view is that of an observer looking at a P–X plane from the right side of Figure 4.) Figure 6a–c corresponds to the isotherms labeled T_1, T_2, and T_3, respectively in Figure 4. The qualitative features of the corresponding K-value diagrams are shown in Figure 6d–f. The horizontal lines in Figure 6, a and b, are tie lines that mark the pressures at which three phases coexist at the fixed temperature of the diagram; these correspond to the vertical dash–dot lines in the K-value plots in Figure 6, d and e. At temperatures T_1 and T_2 there are three distinct two-phase regions, $L^\alpha + L^\beta$, $L^\alpha + V$, and $L^\beta + V$. The liquid–liquid region $L^\alpha + L^\beta$ ends at a critical point C_{LL} in each case. At T_1, below the DME critical temperature, the $L^\beta + V$ region ends at the right side of the diagram at b, a point on the DME vapor pressure curve; at T_2 this region ends in a vapor–liquid critical point C_{VL}, which lies on the critical line C_1–U in Figures 4 and 5. As the temperature T_U is approached from below, the $L^\beta + V$ region in an isothermal diagram diminishes in size and vanishes in a horizontal inflection point (the upper critical end point U) when that temperature is reached. Thus, U is a limiting point at which the L^β and V phases become identical in the presence of the liquid phase L^α. At T_3, between the upper critical end point, U, and the critical

Table III. Experimental Equilibrium Compositions for DME/H_2O[a] in the Liquid-Liquid (L^α-L^β) Region

P, MPa	X_1^α	X_1^β	P, MPa	X_1^α	X_1^β
		T = 100.11 °C			
4.964	0.123	0.745	34.474	0.176	0.611
6.895	0.135	0.735	38.059	0.181	0.582
10.342	0.137	0.717	41.472	0.190	0.558
11.101	0.139	0.712	44.402	0.193	0.506
13.789	0.140	0.703	46.912	0.226	0.471
17.264	0.145	0.681	48.263	0.242	0.457
20.684	0.150	0.665	49.642	0.265	0.450
24.132	0.157	0.642	50.642	0.296	0.391
27.579	0.167	0.630	(50.8)	(0.35)	(0.35)
31.199	0.173	0.622			
		T = 121.06 °C			
7.033	0.126	0.702	38.390	0.218	0.472
14.038	0.140	0.642	41.727	0.241	0.443
20.753	0.153	0.600	43.437	0.256	0.416
24.518	0.172	0.583	44.126	0.264	0.413
27.717	0.179	0.546	(45.1)	(0.34)	(0.34)
34.681	0.199	0.509			
		T = 140.86 °C			
7.253	0.107	0.689	27.579	0.183	0.484
9.653	0.128	0.666	31.026	0.210	0.447
13.831	0.148	0.602	32.585	0.228	0.421
17.375	0.141	0.584	33.474	0.231	0.408
20.684	0.158	0.546	34.301	0.245	0.375
24.173	0.178	0.508	(35.3)	(0.31)	(0.31)
		T = 154.25 °C			
7.239	0.106	0.687	24.132	0.181	0.445
7.805	0.110	0.668	25.855	0.199	0.405
8.963	0.115	0.648	26.476	0.205	0.385
10.756	0.114	0.618	27.731	0.228	0.371
12.273	0.120	0.592	27.820	0.232	0.365
15.168	0.137	0.565	28.282	0.263	0.355
18.685	0.150	0.514	(28.7)	(0.30)	(0.30)
22.063	0.162	0.471			

[a] Mixture critical points (in parentheses) have been estimated by extrapolation of experimental measurements.

Table IV. Three-Phase Line Data for the System DME/H_2O

temp, °C	press., MPa	X_1^α	X_1^β	Y_1
50.00	1.027	0.155	0.814	0.977
75.00	1.800	0.128	0.781	0.958
100.11	2.848	0.104	0.755	0.936
121.06	4.054	0.090	0.727	0.910
127.34	4.440	0.089	0.725	0.901
130.11	4.661	0.087	0.721	0.879
140.85	5.454	0.081	0.705	0.862
150.35	6.219	0.093	0.736	0.844
154.25	6.605	0.104	0.755	0.832

Table V. Low-Pressure Critical Line Data for the System DME/H_2O

temp, °C	press., MPa	DME mole fraction	temp, °C	press., MPa	DME mole fraction
(126.90)[a]	5.27	1.00	150.35	6.4	0.82
127.34	5.3	0.98	154.25	6.6	0.79
130.11	5.4	0.95	(157.00)[b]	6.72	0.78
140.85	5.9	0.87			

[a] Pure-DME critical point. Value obtained from the literature (9). [b] Upper critical end point (UCEP).

point of water, C_2, only a single two-phase region, $L^\alpha + V$, exists. This region diminishes in size with increasing temperature and vanishes at C_2; at higher temperatures only a single fluid phase exists.

An interesting feature of the phase diagram is the presence of a "nose" on the lower right side of the isotherm T_3 in Figure

Table VI. High-Pressure Critical Line Data for the System DME/H_2O

temp, °C	press., MPa	DME mole fraction	temp, °C	press., MPa	DME mole fraction
100.11	50.8	0.35	180.15	21.4	0.28
121.06	45.1	0.34	200.45	17.6	0.27
140.86	35.3	0.31	220.01	15.5	0.26
154.25	28.7	0.30	(374.13)[a]	22.09	0.00
160.05	26.3	0.29			

[a] Pure-water critical point. Value obtained from the literature (8).

6c. The negative slope in the isotherm, just above the maximum in composition, indicates a rapid increase in the solubility of liquid water in supercritical DME with increasing pressure. This nose remains pronounced at temperatures as high as 60 °C above the upper critical end point, indicating enhanced solubility of the condensed phase (H_2O) in the supercritical solvent (DME) over an extended temperature range. This enhanced solubility, associated with the presence of an upper critical end point near the solvent critical point, is important in supercritical extraction; the effect is exaggerated here, because the condensed phase (H_2O) is itself volatile, but it illustrates the phenomenological relationship between critical end points and enhanced solubility in a supercritical fluid.

Registry No. $(CH_3)_2O$, 115-10-6.

Literature Cited

(1) Tsang, C. Y.; Streett, W. B. *J. Chem. Eng. Data* **1981**, *26*, 155.
(2) Chang, E.; Calado, J. C. G.; Streett, W. B. *J. Chem. Eng. Data* **1982**, *27*, 293.
(3) Chang, C. D.; Silvestri, A. J. *J. Catal.* **1977**, *47*, 249.
(4) Harney, B. M.; Mills, A. G. *Hydrocarbon Process.* **1980**, *59*, 67.
(5) Gubbins, K. E.; Streett, W. B. *Chem. Eng. Educ.* **Fall 1981**, 172.
(6) Pozo, M. E.; Streett, W. B. "Proceedings of the Third International Conference on Fluid Properties and Phase Quilibria for Chemical Process Design, Callaway Gardens, GA, April 1983"; *Fluid Phase Equilib.* **1983**, *14*, 219.
(7) Van Konynenberg, P. H.; Scott, R. L. *Philos. Trans. R. Soc. London* **1980**, *298*, 495.
(8) Keenan, H. J.; Keyes, F. G.; Hill, P. G.; Moore, J. G. "Steam Tables"; Wiley: New York, 1969.
(9) Cardoso, E.; Bruno, A. *J. Chem. Phys.* **1923**, *20*, 347.

Received for review September 26, 1983. Accepted March 12, 1984. This work was supported in part by grant CPE 81-04708 from the National Science Foundation. Acknowledgment is also made to the donors of the Petroleum Research Fund, administered by the American Chemical Society, for partial support of this research. M.E.P. acknowledges a generous fellowship from the Venezuelan government through the Fundacion Gran Mariscal de Ayacucho.

Osmotic Coefficients of Water for Thorium Nitrate Solutions at 25, 37, and 50 °C†

Robert J. Lemire,* Norman H. Sagert, and Danny W. P. Lau

Research Chemistry Branch, Whiteshell Nuclear Research Establishment, Atomic Energy of Canada Limited, Pinawa, Manitoba, Canada R0E 1L0

Vapor pressure osmometry was used to measure osmotic coefficients of water for thorium nitrate solutions at 25, 37, and 50 °C and at molalities up to 0.2 mol·kg^{-1}. The data were fitted to three- and four-parameter equations containing limiting-law terms for a 4:1 electrolyte. The variation of the osmotic coefficients as a function of temperature was found to be small. The results are compared to published values for the osmotic coefficients.

Introduction

To analyze the data from experiments determining activities in the $Th(NO_3)_4$–HNO_3–H_2O system at 25 and 50 °C (*1*, *2*), osmotic coefficients were required for the $Th(NO_3)_4$–H_2O system. For 25 °C and low concentrations of thorium nitrate, osmotic coefficients have been reported by Apelblat et al. (*3*) from vapor pressure osmometry and by Robinson and Levien (*4*) from isopiestic measurements. Apelblat et al. (*3*) reported limited sets of osmotic coefficients at 37 and 50 °C, and these values are essentially identical for the two temperatures. Osmotic coefficients can also be calculated for ~0 °C from the freezing point experiments of this same group (*5*). The results of all these experiments (see Figure 1) show no clear pattern in the variation of the osmotic coefficient with temperature. Also, as noted by Apelblat (*3*), the two sets of 25 °C results do not agree well, thus complicating the calculation of thermodynamic properties for Th^{4+}(aq) (*6*, *7*). Therefore, we have reexamined the osmotic coefficients of water for $Th(NO_3)_4$ solutions at 25, 37, and 50 °C by using our modern vapor pressure osmometer.

Experimental Section

Thorium nitrate hydrate was recrystallized from concentrated aqueous solution by the addition of freshly prepared, anhydrous nitric acid. The precipitate was collected, washed with dilute nitric acid, and dried for several weeks under vacuum over anhydrous sodium carbonate. Stock solutions were prepared from this material and from the original, reagent-grade thorium nitrate hydrate. The two solutions were analyzed by titration with standard EDTA solution, and the concentrations were found to be 1.77 ± 0.01 and 2.11 ± 0.01 mol·dm^{-3}, respectively. Aliquots of both stock solutions were diluted to prepare the solutions for the osmotic coefficient measurements. The results obtained by using the reagent-grade thorium nitrate and the recrystallized salt were consistent within the error limits of the osmometric measurements.

Osmotic coefficients were measured at 25, 37, and 50 °C by using a Corona/Wescan Model 232A vapor pressure osmometer. In this instrument, the steady-state temperature difference is measured between a drop of pure water and a drop of solution, both being maintained in a chamber saturated with water vapor. Thermistors are used as temperature sensors, and the difference in the voltage developed across each of the two thermistors, ΔV, is measured at a constant bridge current. The operation of this instrument has been described by Burge (*8*).

At each temperature, the instrument was calibrated by using solutions of mannitol (ACS reagent grade) in water as standards. The voltage difference, ΔV, was divided by the mannitol

† Issued as AECL-8089.

0021-9568/84/1729-0329$01.50/0 © 1984 American Chemical Society